An extended period of episodic northern mid-latitude glaciation on Mars during the Middle to Late Amazonian: Implications for long-term obliquity history

Caleb I. Fassett[1], Joseph S. Levy[2], James L. Dickson[3], and James W. Head[3]
[1]Department of Astronomy, Mount Holyoke College, South Hadley, Massachusetts 01075, USA
[2]Institute for Geophysics, University of Texas, Austin, Texas 787583, USA
[3]Department of Geological Sciences, Brown University, Providence, Rhode Island 02912, USA

ABSTRACT

Mars is the only planet other than Earth in the Solar System that has a preserved nonpolar geological record of glaciation on its surface. Nonpolar ice deposits on Mars have been linked to variations in spin-axis obliquity that cause mobilization of polar ice and redeposition at lower latitudes, forming ice-rich and glacial deposits. Remnant nonpolar glacial deposits are found across the northern mid-latitudes where surface ice is not currently stable, implying that different climatic conditions existed on Mars in the past. Individual glacial deposits are often too small to date reliably using impact crater size-frequency data. We describe a novel approach that allows us to derive new information about when glaciation occurred in broad areas of the northern mid-latitudes. In this region we have classified (1) craters that superpose preexisting glacial deposits and were modified by later accumulation (and therefore formed during an epoch when glaciation was occurring), and (2) craters that are superposed on glacial deposits but are themselves unmodified by ice accumulation (and thus post-date significant glaciation). The sparse population of post-glacial craters reveals that the last period of extensive ice deposition of this type in this latitude band was recent (Late Amazonian). The substantial number of craters formed during the recurring glacial periods implies that northern mid-latitude glaciation was a long-lived recurring process, occurring over a period of at least ~600 m.y. On the basis of Mars atmospheric general circulation models, these results are consistent with higher obliquity being common in the past, with recurring periods of obliquity exceeding the 25° axial tilt of Mars today. These observations support the statistical prediction of J. Laskar and colleagues that the median obliquity during the Amazonian was ~35°–40°.

INTRODUCTION

A range of evidence suggests that widespread ice deposition and local ice flow occurred in the northern mid-latitudes (30°–50°N) of Mars during its history. Evidence includes morphological indicators of ice accumulation and flow (e.g., Squyres, 1979; Lucchitta, 1981; Head et al., 2005, 2006a, 2006b, 2010), remnant ice underlying pedestal craters (e.g., Kadish et al., 2010; Kadish and Head, 2014), and radar observations of buried glacial ice in the subsurface (Holt et al., 2008; Plaut et al., 2009). Among the mid-latitude glacial landforms are features mapped as lineated valley fill, lobate debris aprons, and concentric crater fill. The evidence that these features formed from deposition of snow and ice, which accumulated and flowed (as opposed to ice-assisted creep of debris) was described in Head et al. (2010) and Levy et al. (2010). After glacial flow, most of these landforms underwent postglacial modification and ice loss due to sublimation and formation of a debris cover (e.g., Fastook et al., 2014). The morphology, distribution, and abundance of these different glacial features vary geographically in the northern mid-latitudes, just as individual glaciations on Earth produce different styles (e.g., valley glaciers, regional ice sheets, plateau glaciation) (e.g., Denton and Hughes, 1980; Boulton et al., 1985).

Most of these northern mid-latitude glacial deposits are at latitudes where surface and ground ice is currently unstable (Mellon and Jakosky, 1995). At current obliquity, on flat topography, martian ground ice is generally stable only poleward of ~45° (Mellon and Jakosky, 1995; Aharonson and Schorghofer, 2006). Nonetheless, various observations point to ice remaining present in the shallow subsurface equatorward of this boundary (Plaut et al., 2009; Byrne et al., 2009). This implies that the glacial deposits are relicts of past conditions, possibly from a different spin-orbit configuration (Mellon and Jakosky, 1995; Madeleine et al., 2009). A major question for reconstructing the climate history and geological evolution of Mars is the timing and duration of the period when widespread ice accumulation in these regions was possible.

Earlier studies have focused on determining ages for individual units and features on the basis of their superposed crater population, reporting crater frequencies on glacial unit surfaces consistent with Middle to Late Amazonian ages of ca. 1 Ga to ca. 100 Ma (in the Hartmann, 2005, isochron system) (Mangold, 2003; Levy et al., 2007; Morgan et al., 2009; Baker et al., 2010).

Although useful, the interpretation of these crater retention ages is complicated by several factors: (1) the initial size of the superposed crater may differ depending on whether it penetrates into debris cover or ice (Kress and Head, 2008); (2) post-formation modification of craters may be continuous and ongoing (e.g., Mangold, 2003); and (3) there are few large craters to contribute to robust age determinations as a result of the relatively young ages of the deposits. Furthermore, due to deformation of the active debris-covered glacial surfaces, craters forming during glaciation may be destroyed, and the derived ages document the end of glacial activity at a location, rather than capturing the persistence of mid-latitude glaciation.

We therefore adopt a different strategy. We take two approaches to further constrain the chronology of ice deposition in the northern mid-latitudes. First, we examine all craters with diameter, D, ≥2.5 km between 30°N and 50°N to assess the number of fresh craters stratigraphically superposed on glacial deposits that lack the signature of subsequent glacial modification (e.g., Fig. 1A). The number of these craters provides a bound on how recently ice deposition last occurred on a regional scale. Second, we mapped craters that formed when glacial deposits were already present, but underwent subsequent ice deposition on their interiors (e.g., Fig. 1B). The population of these craters is a function of the time period when glaciation occurred in this area, although the derived period may not be continuous or globally synchronous. For convenience, we refer to craters in the first category as postglacial (interpreted to form after the last period of glaciation) and those in the second category as synglacial (interpreted to form during or between periods of glaciation).

MAPPING METHODS

To analyze the chronology of these deposits, we constructed uncontrolled global mosaics of data from the Mars Reconnaissance Orbiter Context Camera (CTX; see Malin et al., 2007) and Mars Odyssey Thermal Emission Imaging System visible (THEMIS VIS; see Christensen et al., 2004). These mosaics were tiled into 15° × 15° regions and sampled at 18 m/pixel (px), which is the maximum resolution of THEMIS VIS data, and down sampled from the native resolution of CTX (~5 m/px). This provides more than sufficient resolution (>100 px) to

© 2014 Geological Society of America. For permission to copy, contact Copyright Permissions, GSA, or editing@geosociety.org.

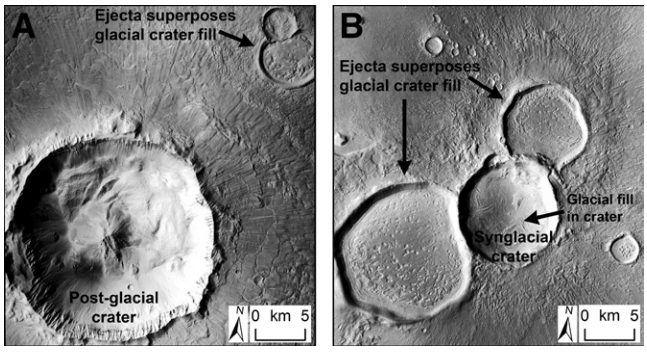

Figure 1. A: Example of 21-km-diameter postglacial crater at 33°N, 118.5°E. The fresh crater lacks glacial fill, but its ejecta is superposed on a crater with preexisting interior glacial fill to its northeast (Mars Reconnaissance Orbiter Context Camera, CTX, image B21_017971_2133). B: Example of 10 km synglacial crater, 32.5°N, 83.3°E. Ejecta from the central crater was deposited on concentric crater fill in neighboring craters, so ice must have been present when the central crater formed. Later deposition occurred in the central crater, implying that it formed during the period of recurring glaciation (CTX images G18_025317_2122 and P17_007516_2128). In both A and B, where the ejecta was deposited onto the surface of preexisting ice-rich crater fill, the surface texture is pitted and deformed, with a ropy and/or loopy appearance. This pitted texture is common where ejecta was deposited onto preexisting ice-rich units. We interpret this texture to be the result of ejecta impacting and disrupting glacial debris cover, possibly leading to local exposures of underlying ice. The surface was then modified by a combination of flow and sublimation, resulting in the observed texture.

recognize and classify the ≥2.5 km craters that are the focus of this study. All NASA Planetary Data System–released THEMIS and CTX data as of 31 January 2013 were included in the mosaics; together, these data cover 95% of the 30°–50°N region.

Using ArcMap (www.esri.com), glacial deposits were mapped at ~1:250,000 scale, although some unit boundaries and regions were mapped at a higher level of detail. To define glacial units, we follow the criteria in Head et al. (2010) and Levy et al. (2010). Typical characteristics of the features we interpret as glacial are: (1) accumulation zones in alcoves, or along crater or massif walls; (2) lobes of material extending downslope from these zones, often with ridges on their surface that can be parallel or transverse to flow. (3) Where flows interact with each other, or with topographic constrictions or openings, folding or deformation is common (attributed to differential ice velocity resulting from these interactions). (4) Pits or depressions are sometimes found on surfaces where differential sublimation may have occurred. (5) A distinctive, knobby surface texture is commonly visible on these surfaces at the scale of Mars Orbiter Camera or HiRISE (High Resolution Imaging Science Experiment) images. (6) Occasionally, moraines or trimlines associated with past glacial highstands are observed.

Mapping results based on applying these criteria are shown in Figure 2. Consistent with earlier studies (Squyres, 1979; Head et al., 2010), ice-rich deposits are concentrated in certain regions and longitudes, especially in northern Tharsis (Tempe Terrae) and northern Arabia (Deuteronilis Mensae). These areas were likely to have been favorable sites for glaciation as a result of having greater topographic relief. This topographic relief may have enhanced both accumulation and preservation of ice beyond what is typical for the latitude band as a whole.

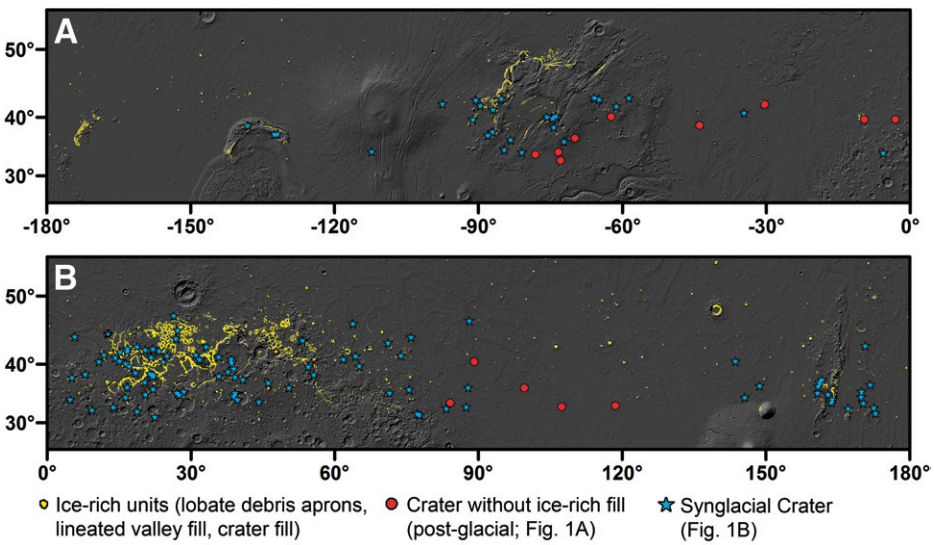

Figure 2. Maps of Mars showing glacial deposits in the northern mid-latitudes (yellow), with locations of postglacial (red) and synglacial craters (blue) (not to scale); only craters within 1 diameter of glacial deposits are shown. Hillshade base map is from Mars Laser Orbiter Altimeter data, and is in Mercator projection. A: Western hemisphere. B: Eastern hemisphere.

Following this mapping, we used the Robbins and Hynek (2012) database of craters on Mars, which is complete to ≥1 km, to systematically examine all craters with $D \geq 2.5$ km to determine if they had glacial deposits on their interior and/or if their ejecta superposed earlier glacial deposits (e.g., Fig. 1). For all mapped craters, we independently measured crater sizes using CraterTools (Kneissl et al., 2011); the relative median difference of our diameter measurements from the Robbins and Hynek (2012) measurements is 3.8%.

A buffered crater counting approach was used to determine the count area for crater statistics (Fassett and Head, 2008). The buffered area in this study is the extent of ice-rich deposits in Figure 2. For a crater to be included in the count, its rim has to be within one crater diameter of this region. The basis for this criterion is the observation that continuous ejecta deposits from craters on Mars characteristically extend at least one crater diameter from their rim (e.g., Melosh, 1989; Barlow, 2005). The assumption here is that a stratigraphic relationship can be determined between the ice-rich unit and craters to a distance of at least one crater diameter beyond their rim.

Using this approach has two advantages over typical crater statistics derived from direct superposition. First, it expands the effective count area, because it takes advantage of the fact that large craters subtend more area than small ones, and stratigraphic determinations are possible over a greater region for large craters than for small ones. Second, this technique allows greater clarity when a large crater is superposed close to the boundary of the ice-rich material because the count area remains easy to define, despite the local burial of preexisting deposits of interest. Both we and others have verified that the buffered crater-counting methodology results in frequencies that are equivalent to more traditional crater counting approaches (Fassett and Head, 2008; Kneissl and Michael, 2013).

RESULTS: TIMING AND PERSISTENCE

The geographic locations of craters that postdate and are interspersed with glacial units are shown in Figure 2, along with the results of our mapping. We also report details of our crater classification in Table 1.

Postglacial Craters

Within 1 crater diameter of the mapped glacial deposits, only 15 postglacial craters larger

TABLE 1. CENSUS OF CRATERS ≤2.5 km IN DIAMETER IN THE 30°N TO 50°N LATITUDE BAND AND CLASSIFIED IN OUR STUDY

A. Number of craters in latitude band, 30°N–50°N	8708
B. Number of craters filled or partially filled by glacial material	3302
C. Number of fresh craters lacking fill in region where glacial units are common	205
D. Number of post-glacial craters, within one crater diameter of glacial units	15
E. Number of synglacial craters, within one crater diameter of glacial units	119

Note: The total area of this band is 19.2×10^6 km^2; in our mapping, 0.35×10^6 km^2 (~2%) is covered by glacial units (crater fill, valley fill, debris aprons). The total number of craters in these latitudes (A) is from Robbins and Hynek (2012). More than 35% of the craters with diameter ≤2.5 km in these latitudes have glacial fill on their interior (B). Many of the craters without ice (in A but not B) predate glaciation (e.g., were degraded and lacked steep slopes allowing substantial accumulation). Only a small percentage of fresh craters are unmodified by ice and located in the broad region where glaciation was common (C). Not all of these craters need to postdate the last glacial episode; some may not have undergone much modification. Thus, we use the statistics (Fig. 3) of postglacial (D) and synglacial craters (E) that have a clear stratigraphic relationship with the glacial material, and are within one crater diameter of the mapped glacial units, to constrain the period of glaciation.

than 2.5 km were observed (Fig. 2). Figure 3A is a plot of the crater size-frequency distribution of these postglacial craters. These data are consistent with an average age of 110 Ma using the Hartmann (2005) chronology. However, because the distribution of postglacial craters is not spatially random (see Fig. 2), this age is an average that masks real spatial variations in when glacial deposition terminated in particular locations. For example, in the 25°–80°E region, the largest postglacial crater we noted within 1 crater diameter of mapped glacial units was ~730 m, despite the fact that glacial deposits are common in this region. Even outside the defined buffer, in the whole of the 25°–80°E, 30°–50°N region, we noted only 2 craters larger than 2.5 km that are candidates to postdate the last episode of glaciation. This low density of craters gives limited statistics for estimating an absolute age, but is consistent with ice accumulation in this region as recently as 20–50 Ma, an age in accord with suggestions based on the density of small superposed craters on the youngest glaciated surface (e.g., Hauber et al., 2005; Baker et al., 2010). Glaciation appears to have occurred less recently in regions such as Acidalia Planitia, Tempe Terra, and Utopia Planitia, where a greater concentration of postglacial craters is observed.

Synglacial Craters

We refer to craters that superpose preexisting glacial deposits and that were subsequently modified by later accumulation on their interior as synglacial (meaning they formed during the period of recurring ice age conditions on Mars). In the northern mid-latitudes, we found 119 synglacial craters within 1 crater diameter of another exposed glacial deposit larger than 2.5 km. Because growth of a crater population is a relatively slow process, the comparatively large number of craters in this category provides strong evidence that glacial units remained preserved at the surface for an extended period of time, and that the period over which glacial episodes occurred was long. The combined synglacial and postglacial population gives an age of ca. 700 Ma in the Hartmann (2005) chronology (Fig. 3B), which implies that ice was at these locations for at least ~600 m.y. (from the ca. 700 Ma model age of the combined population to the ca. 100 Ma model age of the postglacial population). Using the Neukum production function (Ivanov, 2001), this period would be ~1.2 b.y., from 1.4 Ga to 210 Ma. The factor of two difference in age is a result of the systematic difference between the Hartmann (2005) and Neukum (Ivanov, 2001) models, but does not affect any of our qualitative results.

Because the stratigraphic relationship used to recognize synglacial craters may be destroyed as the surface evolves, this estimated period is a minimum duration. Morever, this technique aggregates craters that formed across an epoch when glaciation may have occurred multiple times, and it cannot distinguish continuous glaciation from multiple independent glacial eras during which previously emplaced deposits survived. Regardless of these limitations, our data indicate that a period, or multiple periods, of glaciation occurred over an extended period in the Middle to Late Amazonian in the northern mid-latitudes of Mars.

SUMMARY AND CONCLUSIONS

This evidence for a long-lived era of recurring ice ages in broad areas of the northern mid-latitudes of Mars is consistent with earlier measurements in specific locales (e.g., Head et al., 2005, 2006a, 2006b, 2010; Hauber et al., 2005, 2008; Levy et al., 2007, 2010; Baker et al., 2010). This work, however, represents the first integrated calculation of the period of time when deposition of ice and glaciation across the northern mid-latitudes occurred.

Although some ice has been lost since the glaciation was at its maximum extent (e.g., Dickson et al., 2008; Hauber et al., 2008), the persistence of ice in the martian mid-latitudes is striking, as is the fact that ice remains present in the near subsurface (Holt et al., 2008; Plaut et al., 2009), even at latitudes where it is not in diffusive equilibrium with the atmosphere (Mellon and Jakosky, 1995). Coupled with the fact that deposition of ice in the mid-latitudes is favored at higher obliquity than present (~35°; Madeleine et al., 2009), these observations suggest that the average or typical past climate state during the Middle to Late Amazonian was different from today. Otherwise, the glacial deposits described here and elsewhere (e.g., in the tropics, Head and Marchant, 2003; middle to high latitudes, Head et al., 2003; Kadish et al., 2010; Kadish and Head, 2014) could not have taken place over such an extended period of time.

These results are also consistent with the recent obliquity of Mars being lower than is typical, in comparison to the long-term average

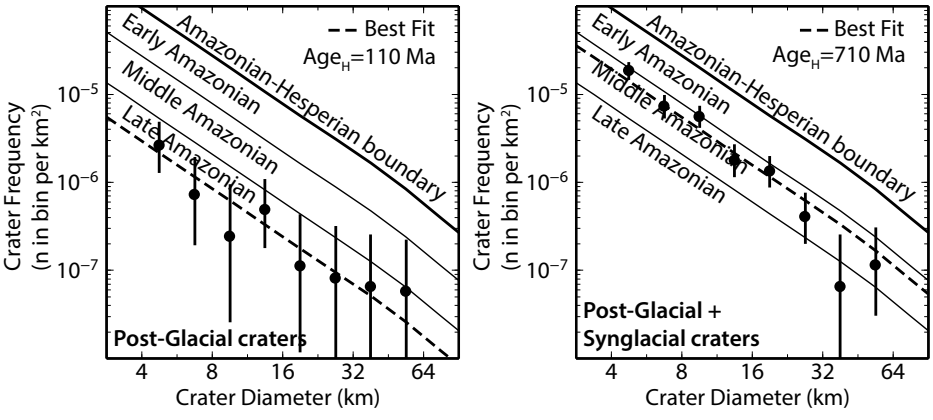

Figure 3. Incremental crater size-frequency plots compared with isochrons from Hartmann (2005). Plotted points are the number of craters in a given size bin per unit area, with the area calculated in a buffer around the mapped glacial deposits shown in Figure 2. A: Frequency of postglacial craters in the buffered area. This is consistent with average Hartmann age of the postglacial population of ca. 110 Ma. Locally, glaciation and ice deposition likely persisted longer (or, conversely, terminated earlier) in particular regions. B: Frequency of postglacial plus synglacial craters in the buffered area. This provides an estimate of minimum age for when first ice deposition must have occurred, since ca. 710 Ma, into at least Middle Amazonian. Estimates for absolute ages are computed by finding the best-fit Hartmann isochron to data using a nonlinear least squares fit, weighted by the inverse of the error in each $\sqrt{2}$ bin.

over much of the Middle to Late Amazonian. This supports Laskar et al.'s (2004) statistical prediction that the long-term average obliquity on Mars (~35° during the past 250 m.y., ~38° over the past 4 b.y.) was higher than its present value (~25°).

ACKNOWLEDGMENTS

Fassett and Levy were supported by National Aeronautics and Space Administration (NASA) Mars Data Analysis program award NNX13AN50G, and Head was supported by NASA Mars Data Analysis program award NNX11AI81G. Donna Jurdy, Nadine Barlow, Stuart Robbins, and an anonymous reviewer provided comments that improved the manuscript.

REFERENCES CITED

Aharonson, O., and Schorghofer, N., 2006, Subsurface ice on Mars with rough topography: Journal of Geophysical Research, v. 111, E11007, doi:10.1029/2005JE002636.

Baker, D.M.H., Head, J.W., and Marchant, D.R., 2010, Flow patterns of lobate debris aprons and lineated valley fill north of Ismeniae Fossae, Mars: Evidence for extensive mid-latitude glaciation in the Late Amazonian: Icarus, v. 207, p. 186–209, doi:10.1016/j.icarus.2009.11.017.

Barlow, N.G., 2005, A review of Martian impact crater ejecta structures and their implications for target properties, *in* Kenkmann, T., et al., eds., Large meteorite impacts III: Geological Society of America Special Paper 384, p. 433–442, doi:10.1130/0-8137-2384-1.433.

Boulton, G.S., Smith, G.D., Jones, A.S., and Newsome, J., 1985, Glacial geology and glaciology of the last mid-latitude ice sheets: Geological Society of London Journal, v. 142, p. 447–474, doi:10.1144/gsjgs.142.3.0447.

Byrne, S., et al., 2009, Distribution of mid-latitude ground ice on Mars from new impact craters: Science, v. 325, p. 1674–1676, doi:10.1126/science.1175307.

Christensen, P.R., et al., 2004, The Thermal Emission Imaging System (THEMIS) for the Mars 2001 Odyssey mission: Space Science Reviews, v. 110, p. 85–130, doi:10.1023/B:SPAC.0000021008.16305.94.

Denton, G.H., and Hughes, T.J., eds., 1980, The last great ice sheets: New York, John Wiley & Sons, 484 p.

Dickson, J.L., Head, J.W., and Marchant, D.R., 2008, Late Amazonian glaciation at the dichotomy boundary on Mars: Evidence for glacial thickness maxima and multiple glacial phases: Geology, v. 36, p. 411–414, doi:10.1130/G24382A.1.

Fassett, C.I., and Head, J.W., 2008, The timing of martian valley network activity: Constraints from buffered crater counting: Icarus, v. 195, p. 61–89, doi:10.1016/j.icarus.2007.12.009.

Fastook, J.L., Head, J.W., and Marchant, D.R., 2014, Formation of lobate debris aprons on Mars: Assessment of regional ice sheet collapse and debris-cover armoring: Icarus, v. 228, p. 54–63, doi:10.1016/j.icarus.2013.09.025.

Hartmann, W.K., 2005, Martian cratering 8: Isochron refinement and the chronology of Mars: Icarus, v. 174, p. 294–320, doi:10.1016/j.icarus.2004.11.023.

Hauber, E., et al., 2005, Discovery of a flank caldera and very young glacial activity at Hecates Tholus, Mars: Nature, v. 434, p. 356–361, doi:10.1038/nature03423.

Hauber, E., van Gasselt, S., Chapman, M.G., and Neukum, G., 2008, Geomorphic evidence for former lobate debris aprons at low latitudes on Mars: Indicators of the Martian paleoclimate: Journal of Geophysical Research, v. 113, E02007, doi:10.1029/2007JE002897.

Head, J.W., and Marchant, D.R., 2003, Cold-based mountain glaciers on Mars: Western Arsia Mons: Geology, v. 31, p. 641–644, doi:10.1130/0091-7613(2003)031<0641:CMGOMW>2.0.CO;2.

Head, J.W., Mustard, J.F., Kreslavsky, M.A., Milliken, R.E., and Marchant, D.R., 2003, Recent ice ages on Mars: Nature, v. 426, p. 797–802, doi:10.1038/nature02114.

Head, J.W., et al., 2005, Tropical to mid-latitude snow and ice accumulation, flow and glaciation on Mars: Nature, v. 434, p. 346–351, doi:10.1038/nature03359.

Head, J.W., Marchant, D.R., Agnew, M.C., Fassett, C.I., and Kreslavsky, M.A., 2006a, Extensive valley glacier deposits in the northern mid-latitudes of Mars: Evidence for late Amazonian obliquity-driven climate change: Earth and Planetary Science Letters, v. 241, p. 663–671, doi:10.1016/j.epsl.2005.11.016.

Head, J.W., Nahm, A.L., Marchant, D.R., and Neukum, G., 2006b, Modification of the dichotomy boundary on Mars by Amazonian mid-latitude regional glaciation: Geophysical Research Letters, v. 33, L08S03, doi:10.1029/2005GL024360.

Head, J.W., Marchant, D.R., Dickson, J.L., Kress, A.M., and Baker, D.M., 2010, Northern mid-latitude glaciation in the Late Amazonian period of Mars: Criteria for the recognition of debris-covered glacier and valley glacier landsystem deposits: Earth and Planetary Science Letters, v. 294, p. 306–320, doi:10.1016/j.epsl.2009.06.041.

Holt, J.W., et al., 2008, Radar sounding evidence for buried glaciers in the southern mid-latitudes of Mars: Science, v. 322, p. 1235–1238, doi:10.1126/science.1164246.

Ivanov, B.A., 2001, Moon cratering rate ratio estimates: Space Science Reviews, v. 96, p. 87–104, doi:10.1023/A:1011941121102.

Kadish, S.J., and Head, J.W., 2014, The ages of pedestal craters on Mars: Evidence for a late-Amazonian extended period of episodic emplacement of decameters-thick mid-latitude ice deposits: Planetary and Space Science, v. 91, p. 91–100, doi:10.1016/j.pss.2013.12.003.

Kadish, S.J., Head, J.W., and Barlow, N.G., 2010, Pedestal crater heights on Mars: A proxy for the thicknesses of past, ice-rich, Amazonian deposits: Icarus, v. 210, p. 92–101, doi:10.1016/j.icarus.2010.06.021.

Kneissl, T., and Michael, G., 2013, Crater size-frequency measurements on linear features—Buffered crater counting in ArcGIS: Proceedings, 44th Lunar and Planetary Science Conference: Lunar and Planetary Institute Contribution 1719, abs. 1079.

Kneissl, T., van Gasselt, S., and Neukum, G., 2011, Map-projection-independent crater size-frequency determination in GIS environments—New software tool for ArcGIS: Planetary and Space Science, v. 59, p. 1243–1254, doi:10.1016/j.pss.2010.03.015.

Kress, A.M., and Head, J.W., 2008, Ring-mold craters in lineated valley fill and lobate debris aprons on Mars: Evidence for subsurface glacial ice: Geophysical Research Letters, v. 35, L23206, doi:10.1029/2008GL035501.

Laskar, J., Correia, A.C.M., Gastineau, M., Joutel, F., Levrard, B., and Robutel, P., 2004, Long-term evolution and chaotic diffusion of the insolation quantities of Mars: Icarus, v. 170, p. 343–364, doi:10.1016/j.icarus.2004.04.005.

Levy, J.S., Head, J.W., and Marchant, D.R., 2007, Lineated valley fill and lobate debris apron stratigraphy in Nilosyrtis Mensae, Mars: Evidence for phases of glacial modification of the dichotomy boundary: Journal of Geophysical Research, v. 112, E08004, doi:10.1029/2006JE002852.

Levy, J., Head, J.W., and Marchant, D.R., 2010, Concentric crater fill in the northern mid-latitudes of Mars: Formation processes and relationships to similar landforms of glacial origin: Icarus, v. 209, p. 390–404, doi:10.1016/j.icarus.2010.03.036.

Lucchitta, B.K., 1981, Mars and Earth: Comparison of cold-climate features: Icarus, v. 45, p. 264–303, doi:10.1016/0019-1035(81)90035-X.

Madeleine, J.-B., Forget, F., Head, J.W., Levrard, B., Montmessin, F., and Millour, E., 2009, Amazonian northern mid-latitude glaciation on Mars: A proposed climate scenario: Icarus, v. 203, p. 390–405, doi:10.1016/j.icarus.2009.04.037.

Malin, M.C., et al., 2007, Context Camera investigation on board the Mars Reconnaissance Orbiter: Journal of Geophysical Research, v. 112, E05S04, doi:10.1029/2006JE002808.

Mangold, N., 2003, Geomorphic analysis of lobate debris aprons on Mars at Mars Orbiter Camera scale: Evidence for ice sublimation initiated by fractures: Journal of Geophysical Research, v. 108, p. 8021, doi:10.1029/2002JE001885.

Mellon, M.T., and Jakosky, B.M., 1995, The distribution and behavior of Martian ground ice during past and present epochs: Journal of Geophysical Research, v. 100, p. 11781–11799, doi:10.1029/95JE01027.

Melosh, H.J., 1989, Impact cratering: A geologic process: New York, Oxford University Press, 245 p.

Morgan, G.A., Head, J.W., and Marchant, D.R., 2009, Lineated valley fill (LVF) and lobate debris aprons (LDA) in the Deuteronilus Mensae northern dichotomy boundary region, Mars: Constraints on the extent, age and episodicity of Amazonian glacial events: Icarus, v. 202, p. 22–38, doi:10.1016/j.icarus.2009.02.017.

Plaut, J.J., Safaeinili, A., Holt, J.W., Phillips, R.J., Head, J.W., Seu, R., Putzig, N.E., and Frigeri, A., 2009, Radar evidence for ice in lobate debris aprons in the mid-northern latitudes of Mars: Geophysical Research Letters, v. 36, L02203, doi:10.1029/2008GL036379.

Robbins, S.J., and Hynek, B.M., 2012, A new global database of Mars impact craters ≥1 km: 1. Database creation, properties, and parameters: Journal of Geophysical Research, v. 117, E05004, doi:10.1029/2011JE003966.

Squyres, S.W., 1979, The distribution of lobate debris aprons and similar flows on Mars: Journal of Geophysical Research, v. 84, p. 8087–8096, doi:10.1029/JB084iB14p08087.

Manuscript received 24 April 2014
Revised manuscript received 10 June 2014
Manuscript accepted 11 June 2014

Printed in USA